Petroleum Science 20 (2023) 3273–3279

Contents lists available at ScienceDirect

Petroleum Science

journal homepage: www.keaipublishing.com/en/journals/petroleum-science

Short Communication

Shale porosity measurement by the saturated oil method: Removing the contribution from oils dissolved in kerogen

Jin-Bu Li [a, b, c], Min Wang [a, *], Hao-Ming Shao [a], Ming Li [a], Liang Liu [a], Shuang-Fang Lu [a, d]

[a] National Key Laboratory of Deep Oil and Gas, China University of Petroleum (East China), Qingdao 266580, Shandong, China
[b] Shaanxi Key Laboratory of Petroleum Accumulation Geology, Xi'an 710000, Shaanxi, China
[c] Key Laboratory of Tectonics and Petroleum Resources (China University of Geosciences), Ministry of Education, Wuhan 430074, Hubei, China
[d] Sanya Offshore Oil & Gas Research Institute, Northeast Petroleum University, Sanya 572025, Hainan, China

ARTICLE INFO

Article history:
Received 7 September 2022
Received in revised form
17 November 2022
Accepted 5 July 2023
Available online 6 July 2023

Edited by Jie Hao and Teng Zhu

Keywords:
Shale
Porosity
Oil saturation
Kerogen-dissolved oil
Water saturation

ABSTRACT

Shale porosity measurements have crucial scientific and economical applications in unconventional petroleum systems. As a standard technique, liquid saturation methods, including water saturation (WS) and oil saturation (OS), have been widely used to measure the porosity of many rock types. For clay-rich shale reservoirs with high organic matter content, it is well known that the WS method may cause clay swelling and induce structural changes in the pore system. The OS method affects the accuracy of porosity measurements because of some of the oil being dissolved by kerogen within the shale; however, this has not received sufficient research attention. In this study, we compare the previously reported and newly tested OS porosities with helium (He) expansion porosity. Results show that OS porosity generally exceeds the He porosity. Furthermore, the higher the total organic carbon (TOC) content and lower the maturity of shale, the greater the difference between the OS and helium porosities. When using the OS method, the effect of kerogen-dissolved oil causes an overestimation of the shale porosity by ~30%. To the best of our knowledge, this is the first time to note the kerogen-dissolve oil effects on OS porosity. Herein, we propose a new, simple, and effective correction method for estimating OS porosity that involves subtracting the kerogen-dissolved oil content from raw OS porosity. In addition, the quantification model of kerogen-dissolved oil capacity is established, taking into account the abundance and maturity of organic matter. Taking the He porosity as the benchmark, the absolute error of the corrected OS porosity does not exceed 1% and the average relative error is only ~10%. The obtained results can help improve the accuracy of shale porosity evaluation methods.

1. Introduction

Porosity measurement has always been a key parameter in oil and gas reserve, reservoir as well as carbon dioxide (CO_2) storage evaluation. Fluid injection techniques, including gas expansion, liquid saturation or immersion, gas adsorption, and mercury intrusion porosimetry, are currently used to directly measure rock porosity (Anovitz and Cole, 2015). Amoung them, gas adsorption and mercury intrusion methods have limited resolutions in shale pore size (e.g., gas adsorption detects pores < 200 nm and mercury intrusion method detects pores > 7 nm) (Josh et al., 2012; Al Hinai et al., 2014; Anovitz and Cole, 2015). The gas expansion method developed by the Gas Research Institute (GRI), employing Boyle's law and injecting gas (e.g., helium) into the rock for testing pore volume, is considered one of the most accurate methods for measuring porosity in low-permeability rocks (Luffel and Guidry, 1992; Anovitz and Cole, 2015). In liquid saturation methods, rock porosity is determined by saturating a clean, dry sample with a liquid of known density. The pore volume of the sample is calculated based on the weight difference between the fully saturated and dry states, and the bulk volume is determined by immersing the sample in liquid and using the Archimedes' Principle. Compared with the He approach, the saturated fluid method not only provides rock porosity value, but also provides pore structure and fluid information when the fluid-saturated sample is further subjected to NMR tests. The key factor considered is the choice of

* Corresponding author.
E-mail address: wangm@upc.edu.cn (M. Wang).

https://doi.org/10.1016/j.petsci.2023.07.006

saturating fluid. Commonly used saturating fluids are water and oil. Kuila et al. (2014) proposed the water immersion porosimetry (WIP) method for measuring gas shale porosity. Lately, many scholars have believed that WIP causes clay mineral swelling, thereby destroying shale pore structures (Topór et al., 2016; Ai et al., 2021; Zhao et al., 2021), and they have recommended brine as a saturating fluid. However, Zhou et al. (2021) reported that shale breaks into slag after saturation with brine. In addition, brine may not be able to enter the organic pores and for mature shale with high TOC, the water or brine saturation (WS) porosity is smaller than the gas porosity (Saidian et al., 2014).

To avoid these issues, some scholars recommend saturating shale samples with light kerosene or n-dodecane (n-C_{12}) to measure porosity (Gannaway, 2014; Kausik et al., 2014; Ousseini Tinni, 2015; Zhang et al., 2017). In our previous studies, we proposed an NMR method for evaluating shale porosity and pore-size distribution based on the differences in T_2 spectra between the fully n-dodecane (n-C_{12}) saturated and dry states of the samples (Li et al., 2019a, 2019b). In this work, although shale porosities determined using the oil saturation (OS) method show an excellent correlation with the NMR method, both methods do not consider the effect of kerogen-dissolved oil. During the oil imbibition process, a portion of the oil enters the kerogen skeleton (Fig. 1) because of the oil-absorbing properties of kerogen polymers and the strong interaction between kerogen and organic solvents (DiStefano et al., 2019), which has been confirmed by geochemists studying kerogen characteristics (Ritter, 2003; Kelemen et al., 2006). Oil imbibition/dissolution into the kerogen skeleton increases the mass of the oil-saturated samples but does not contribute to the porosity of the rock. This causes an overestimation of OS porosity. As reported by scholars, porosity determined using the OS method is generally larger than that obtained using the He method (Fig. 2). In particular, the lower the maturity and the higher the TOC of the kerogen, the greater the amount of oil it absorbs (Jarvie, 2014), increasing the porosity difference between the two methods.

The He approach has been identified as a standard method for measurement of shale porosity according to the Chinese National Standard GB/T34533-2017. Herein, we consider helium porosity as the benchmark and propose an OS porosity correction model considering the oil dissolution effect by different thermally matured kerogens. Subsequently, the model is validated using the new porosity data and the porosity data from previous studies. We hope this provides new perspectives for the accurate measurement of shale porosity.

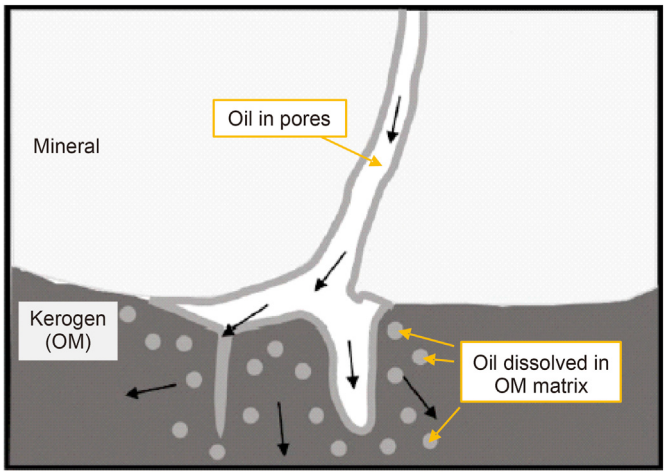

Fig. 1. Schematic of oil occurrence in pores and organic matter matrix in shale sample (modified after Zhu et al., 2020).

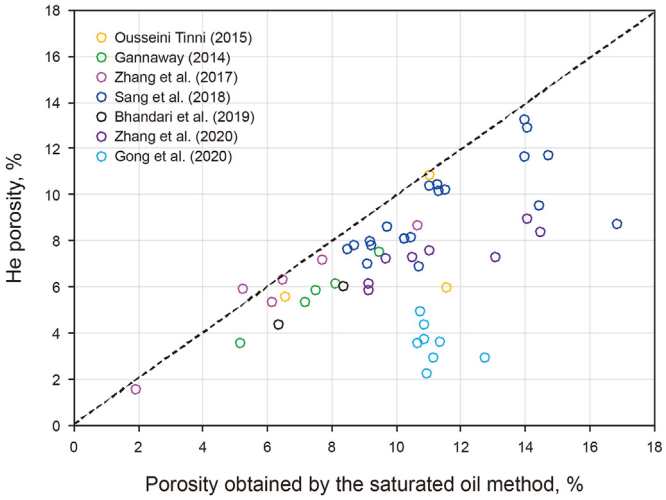

Fig. 2. Porosity comparison between gas expansion and oil saturation methods reported by previous studies (Gannaway, 2014; Ousseini Tinni, 2015; Zhang et al., 2017, 2020; Sang et al., 2018; Bhandari et al., 2019; Gong et al., 2020).

2. Samples and methods

2.1. Samples

A total of 15 shale core samples were selected from the first member of the Qingshankou Formation in the Gulong Sag, Songliao Basin, Eastern China. The shale oil reserves in the Gulong Sag are approximately 1.268 billion tons, successfully developed in recent years. For the selected samples, thermal maturity (vitrinite reflectance, $\%R_o$) is between 0.79% and 1.65%, the total organic carbon content (TOC) ranges from 0.1 to 9.35 w.t.%, and the organic matter is mainly dominated by type II kerogen. Minerals mainly comprise clay minerals (av. ~38%), quartz (~22%), dolomite (18%), and plagioclase (~11%). Clay minerals mainly comprise illite (~51%) and mixed-layer illite/montmorillonites (~36%). The geochemical characteristics and mineral composition of each sample are presented in Table 1.

2.2. Methods

(1) Workflow

Fifteen core plugs with a diameter of ~2.5 cm and height of 3–5 cm were obtained via wire cutting. Each plug was extracted, submitted to He porosity measurement, and saturated with oil (n-dodecane, n-C_{12}) for OS porosity measurement.

Among the 15 core samples, seven were subjected to kerogen isolation. The dissolved oil (n-C_{12}) experiment of increasingly mature kerogen was performed to determine the oil-dissolving capacity of organic matter, which was applied for correcting OS porosity. The OS and He porosities were compared to verify the model. The evaluation process is shown in Fig. 3.

(2) Experiments

a. He porosity measurement (φ_{He}):

The as-received shales were subjected to chloroform extraction for 4 weeks and dried at 65 °C for 12 h to remove the residual fluids. Before the gas porosity measurement, the diameter and height of each plug were

Table 1
Geochemistry and mineral composition of shale samples used in this study.

No.	R_o, %	TOC, w.t.%	Mineral composition, %							Clay components, %			
			Clay	Quartz	Plagioclase	Calcite	Dolomite	Pyrite	Others	I/S	It	K	C
1	0.79	9.35	34.2	16.8	13.4	0.0	24.9	6.4	4.3	46	49	3	2
2*	0.83	2.67	14.9	12.5	4.0	0.0	60.4	5.1	3.1	–	–	–	–
3*	0.94	2.45	20.7	8.1	2.1	0.0	61.3	3.4	4.4	–	–	–	–
4	1.03	3.51	–	–	–	–	–	–	–	–	–	–	–
5*	1.05	1.41	52.9	21.5	13.2	1.1	6.4	2.7	2.2	42	56	0	2
6	1.09	5.61	–	–	–	–	–	–	–	–	–	–	–
7*	1.21	1.67	41.8	24.4	15.5	5.4	0.0	5.9	7.0	34	57	0	9
8*	1.24	2.61	47.8	30.2	8.5	5.8	1.7	3.4	2.6	44	40	6	10
9	1.26	2.83	45.3	22.0	10.2	0.0	14.4	2.8	5.3	44	54	2	0
10	1.32	2.56	45.0	20.3	12.7	3.1	0.9	10.5	7.5	40	47	4	9
11*	1.37	3.75	51.4	25.9	10.3	6.7	0.0	5.7	0.0	38	45	7	10
12	1.41	0.10	30.0	0.0	20.7	4.8	0.0	0.0	44.5	17	48	0	35
13	1.61	2.56	51.7	26.1	14.9	0.0	5.7	0.0	1.6	29	59	3	9
14	1.63	1.22	22.5	9.4	5.3	3.8	42.9	10.0	6.1	–	–	–	–
15*	1.65	2.15	45.6	24.8	13.4	0.0	8.4	5.2	2.6	34	56	0	10

Note: * Represent the samples for kerogen isolation; "—" represent no data analysis; "I/S" represents mixed-layer illite/montmorillonites, "It" represents illite, and "K" and "C" represent kaolinite and chlorite, respectively.

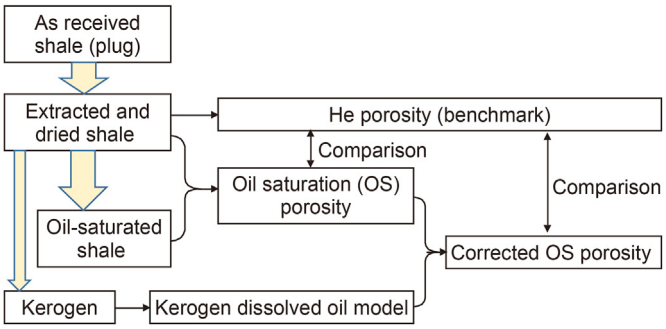

Fig. 3. Brief workflow of the evaluation process.

measured using a vernier caliper for calculating the bulk volume V. The helium porosity measurements were performed using a PoroPDP-200 porosimeter produced by CoeLab, USA.

b. Pressurized saturated oil experiment

After He porosity measurements, dried shales were weighed (m_1) and vacuumed for 24 h, and saturated with n-C_{12} for 72 h at a fluid pressure of 15 MPa. After saturation, the samples were weighed again (m_2). The detailed procedure of the saturation experiment can be found in our previous study (Li et al., 2019a). Shale porosity obtained using the OS method (φ_{os}) is given as follows.

$$\varphi_{os} = \frac{m_2 - m_1}{\rho_o \times V} \times 100\%, \quad (1)$$

where ρ_o is the density of the saturating fluid (n-C_{12}) in g/cm^3 and V is the bulk volume of sample in cm^3.

c. Kerogen-dissolved oil quantification

Kerogen separation was performed by the traditional acid digestion method recorded in the Chinese National Standard GB/T19144-2010. In this work, the shale core samples were crushed to less than 200 mesh, and then treated with the HCl solution for 48 h to remove carbonates. After that, solid residue was collected by filter paper and then dried in an oven overnight at a temperature of 60 °C. Then, the HF and HCl mixture solution (1:1) was used to remove silicates. Subsequently, the extractable organic matter was removed by Soxhlet extraction using toluene as organic solvent. After the above procedures, kerogen was obtained.

Each isolated kerogen sample was poured into a stoppered glass tube with quartz wool at the bottom. The initial height (H_1) of kerogen was measured using a vernier caliper. The tube was immersed into n-C_{12} (25 °C, 72 h) and centrifuged at 8000 rpm for 60 min to remove the bulk fluids between the kerogen particles (Sun et al., 2019). After centrifugation, kerogen height was recorded again as H_2. The kerogen swelling ratio was calculated using the ratio of the two heights. After that, the dissolved oil of kerogen was accordingly quantified as follows (Wei et al., 2012).

$$Q_v = \frac{H_2}{H_1}, \quad (2)$$

$$M_d = \frac{(Q_v - 1) \times \rho_o}{\rho_k \times TOC_k}, \quad (3)$$

where H_1 is the initial height of kerogen in mm; H_2 is the height of kerogen after centrifuge in mm; ρ_o and ρ_k are the densities of n-C_{12} and kerogen, respectively in g/cm^3; TOC_k is total organic carbon content of kerogen, w.t.%; and M_d is the dissolved oil content of kerogen in g oil/g TOC.

3. Results and discussions

3.1. Shale porosity

The porosities measured using the helium method (φ_{He}) and the oil saturation method (φ_{os}) are listed in Table 2 φ_{He} ranges from 2.58% to 11.84%, with an average of 7.94%. Fig. 4a shows the relationship between He porosity and mineral content. φ_{He} is positively correlated with clay minerals and quartz; however, it is negatively correlated with dolomite, indicating that the inorganic pores of shale are mainly attributed to clay pores and quartz intergranular pores. Previous studies reported that the carbonate minerals in Gulong shale are concentrated in the ostracod limestone, and in the silty laminae within fine sandstone and mudstone, calcite and iron cement can be seen filling in between debris particles as well as some residual intergranular pores (Liu et al., 2018; Bai et al., 2022), thus decrease the porosity. In general, the porosity of shale with high maturity and well-developed organic pores positively correlates with the TOC (Milliken et al., 2013). Because of the wide maturity range of the selected samples used in this study, the correlation between He porosity and TOC is complex (Fig. 4b).

Table 2
Porosity comparison between He expansion and oil saturation methods.

No.	Bulk density, g/cm^3	φ_{He}, %	Saturated oil method			Corrected saturated oil method		
			φ_{os}, %	Absolute error, %	Relative error, %	φ_{os-c}, %	Absolute error, %	Relative error, %
1	2.16	5.79	10.74	4.95	85.49	4.27	1.52	26.21
2	2.56	3.33	5.66	2.33	69.97	3.65	0.32	9.55
3	2.66	2.98	4.47	1.49	50.00	2.92	0.06	2.03
4	2.44	8.26	10.58	2.32	28.09	8.92	0.66	8.05
5	2.43	11.84	12.02	0.18	1.52	11.01	0.83	7.02
6	2.34	11.62	13.64	2.02	17.38	11.42	0.20	1.70
7	2.49	10.59	10.60	0.01	0.09	10.57	0.02	0.20
8	2.44	9.68	11.39	1.71	17.67	10.58	0.90	9.31
9	2.57	5.90	8.41	2.51	42.54	7.52	1.62	27.47
10	2.45	9.00	10.18	1.18	13.11	9.50	0.50	5.54
11	2.40	10.12	11.82	1.70	16.80	10.94	0.82	8.14
12	2.50	7.66	8.50	0.84	10.97	8.48	0.82	10.67
13	2.41	9.48	11.34	1.86	19.62	10.97	1.49	15.71
14	2.78	2.58	2.76	0.18	6.98	2.56	0.02	0.76
15	2.52	10.28	8.06	–	–	7.76	2.52	24.51
Min	2.16	2.58	2.76	0.01	0.09	2.56	0.02	0.20
Max	2.78	11.84	13.64	4.95	85.49	11.42	2.52	27.47
Average	2.48	7.94	9.34	1.66	27.16	8.07	0.82	10.46

Note: "–" represents non valid data.

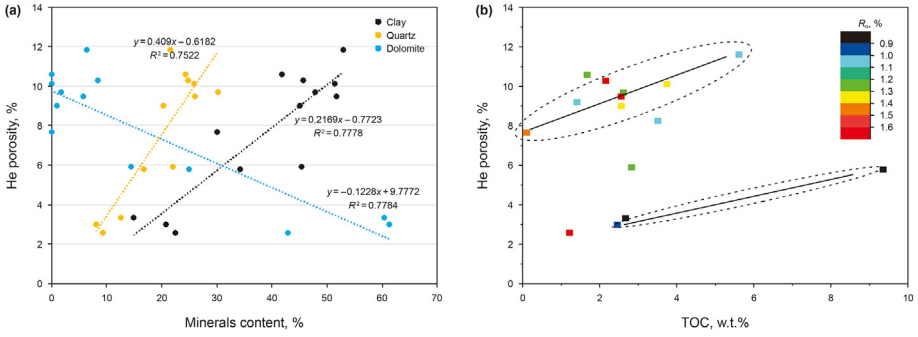

Fig. 4. Relationships between He porosity and (a) mineral composition and (b) TOC content.

Overall, moderately mature (R_o< 1.0%) and highly mature shale (R_o > 1.0%) show positive correlations between He porosity and TOC. The slope of the latter line is steeper, indicating that more organic pores are developed in the shales with higher maturity.

The porosity measured by the oil saturation method (φ_{os}) ranges from 2.76% to 13.64%, with an average of 9.34%. Except for sample No. 15, φ_{os} values are greater than φ_{He} values (Fig. 5), confirming previous reports (Fig. 2). Moreover, the deviation between φ_{os} and φ_{He} increases with increasing TOC. Setting shale porosity measured by the He method as the benchmark, porosity determined via the oil saturation method is overestimated by 0.01%–4.95% (average = 1.66%). The relative errors of the two methods range from 0.01% to 85.49%, with an average of 27.16% (Table 2). That is, kerogen-dissolved oil causes an overestimation of shale porosity by ~30%. Furthermore, the higher the TOC and the lower the maturity of shale samples (e.g., Nos. 1–3, 6), the higher the overestimation of porosity using the oil saturation method. For shale samples with low TOC (e.g., Nos. 7, 12), φ_{os} is almost equal to φ_{He}.

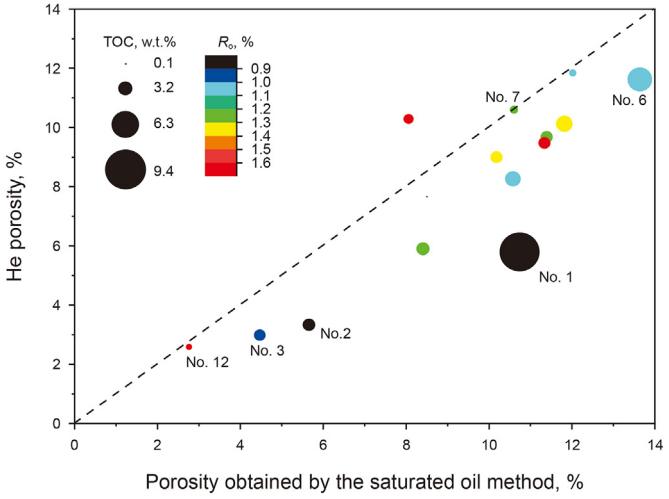

Fig. 5. Cross-plot of He porosity and oil saturation porosity.

3.2. Dissolved oil capacity of kerogen

The swelling ratio of seven kerogen samples (%R_o, 0.83%–1.65%) ranges from 1.045 to 1.232, with an average of 1.098. As the maturity increases, the swelling ratio decreases. A similar trend was reported by Wei et al. (2012), who investigated the swelling of variably matured kerogens obtained from the gold tube thermal simulation experiments. The dissolved oil capacity of kerogen is mainly controlled by the kerogen structure. With increasing maturity, the aromatization degree and crosslink density of kerogen increase (Larsen et al., 2002), reducing the capacity to dissolve oil. According to dissolved oil experiments of kerogen reported by previous scholars (Kelemen et al., 2006; Wei et al., 2012)

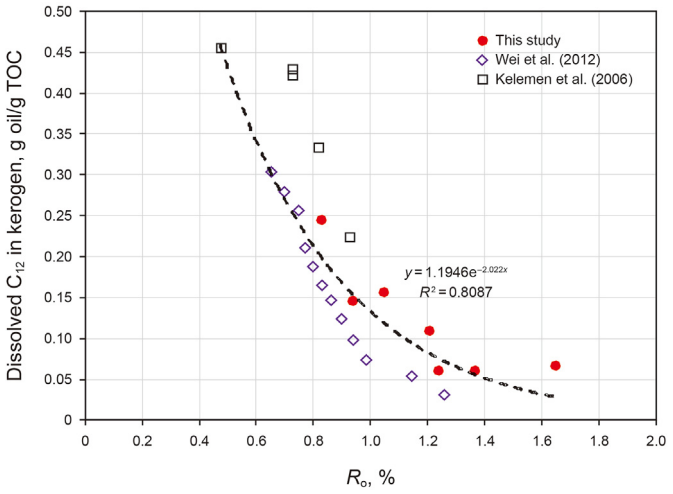

Fig. 6. Relationship between kerogen maturity and dissolved oil capacity.

and test results of this study (Fig. 6), we conclude that the thermal maturity ranges from 0.5% to 1.65% and the dissolved oil capacity of kerogen is ~0.45–0.05 g oil/g TOC. Kerogen-dissolved oil capacity (M_d, g oil/g TOC) can be expressed as follows.

$$M_d = 1.1946 \times e^{-2.022 \times R_o}. \quad (4)$$

3.3. OS porosity correction

In the process of oil saturation, owing to the effect of kerogen-dissolved oil, the weight difference between saturated shale and dried shale is higher than that of the oil entering the pores, causing overestimation of OS porosity. Therefore, the amount of oils dissolved in kerogen should be deducted when using the oil saturation method for measuring shale porosity. Combining Eqs. (1) and (4), the OS porosity should be corrected as follows.

$$\varphi_{os-c} = \frac{m_2 - m_1 - \frac{m_1 \times TOC \times M_d}{100}}{\rho_o \times V} \times 100\% = \varphi_{os} - 1.1946 \times e^{-2.022 \times R_o} \times TOC \times \frac{\rho_b}{\rho_o}, \quad (5)$$

where φ_{os-c} is the corrected porosity obtained using the saturated oil method in % and ρ_b is the bulk density of the shale sample in g/cm^3.

Based on the TOC and maturity data of the 15 shale samples used in this study, the corrected OS porosity ranges from 2.56% to 11.42%, with an average of 8.07%. It is in good agreement with corrected OS and He porosities, with an average absolute porosity error of no more than 1% and a relative error of only ~10% (Table 2). Some samples still have high relative errors even if the corrected OS method is used, such as No.1 and No.9, whose error exceed 25%. Considering that the error of these two samples is high when using the OS method, the relative error may be caused by sample heterogeneity.

In addition, by combining the data of He porosity, OS porosity, TOC, and maturity reported by previous studies, the OS porosity can be corrected via Eq. (5). Furthermore, a good agreement is found between the corrected OS porosity and He porosity (Fig. 7a), and these porosities are distributed on both sides of the diagonal (1:1), with an absolute error not exceeding 2%. The linear correlation coefficient is 85%, further proving the reliability of the correction model.

3.4. Uncertain analysis

There are two key factors when studying shale porosity using the fluid saturation method: one is the aforementioned choice of saturating fluid and the other is the pretreatment of the samples (Kuila et al., 2014). All porosimetry techniques involve removing naturally occurring formation fluids in the as-received shale cores before saturating the pore system with a measurable volume of external fluids. Unlike gas shale, oil-bearing shale samples have relatively low-maturity and high-viscosity fluids, and a small pore throat system. Thus, oil-bearing shales should be crushed first (i.e., GRI method) and extracted using a relatively strong polar solvent for a long time, such as 4 weeks, as recommended by Handwerger et al. (2011). For extraction, chloroform and toluene (or dichloromethane and methanol, 93:7) are the most commonly used solvents and can extract most of the soluble organic matter, causing substantial pore-space recovery (Zargari et al., 2015). The solvent extraction process extracts the oil components generated by and dissolved in kerogen; however, if the sample pretreatment is not thorough, kerogen-dissolved oil remains in the shale before the saturation process, preventing the solvent from entering the kerogen. Besides, kerogen will expands in volume after oil absorption, resulting in reduced pore volume. However, this was not considered in this work. There are some minor errors between the corrected OS and He porosities because of the heterogeneous and complex nature of the shale composition and pores. The errors in shale plug volume and mass measurements could also affect the porosity values, and the possible sources of uncertainty related to shale porosity were discussed in detail by Yang et al. (2016).

The shale TOC can be used to roughly correct the OS porosity when the maturity and bulk density of the shales are unknown. Sandvik et al. (1992) proposed that the S_1 retention capacity of kerogen is 0.1 g HCs/g TOC. Considering the heavy hydrocarbons in pyrolysis S_2 peak, the oil (bitumen "A" extracts) retention capacity of kerogen is ~0.2 g oil/g TOC (Wang et al., 2019). Using this value, we roughly corrected the OS porosity of this study and previously reported data, as shown in Fig. 7b. Except for the relatively large deviations of a few samples from the studies performed by Zhang et al. (2020) and Gong et al. (2020), the correction results show good consistency with the He porosity, and the two are evenly distributed on both sides of the diagonal.

4. Conclusions

In a comparison between OS and He porosities of newly tested 15 shale core samples and previously reported results, the following two observations were made.

(1) OS porosity exceeds the He porosity. The lower the maturity and the higher the TOC of the shales, the greater the difference between the two porosities.
(2) A correction model for OS porosity is proposed using the TOC and maturity data of the core samples. The corrected OS porosity is consistent with the He porosity. When the shale maturity is unknown, a kerogen-dissolved oil capacity of 0.2 g oil/g TOC is recommended to roughly correct the OS porosity.

Declaration of competing interest

The authors declare that they have no known competing

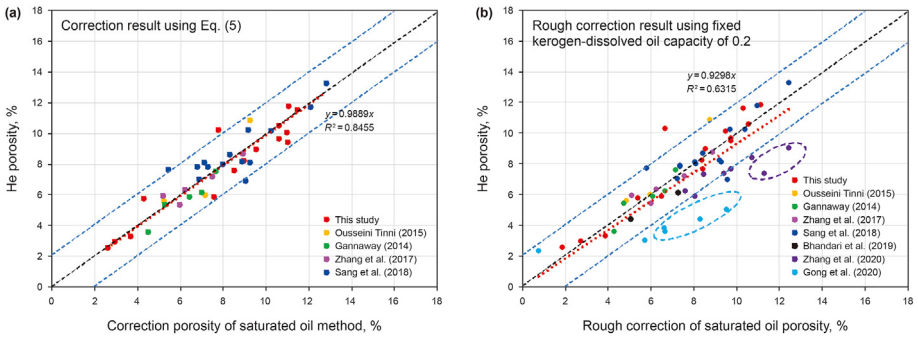

Fig. 7. Cross-plot between He porosity and corrected porosities of oil saturation method considering kerogen-dissolved oil effect. (a) Corrected method using Eq. (5) and (b) roughly corrected method using fixed kerogen-dissolved oil capacity of 0.2.

financial interests or personal relationships that could have appeared to influence the work reported in this paper.

Acknowledgments

This study was funded by the National Natural Science Foundation of China (42102154, 41922015, 42072147), Postdoctoral Research Foundation of China (2021M690168), Postdoctoral Innovative Talent Support Program of Shandong Province (SDBX2021004), Open Fund of Shaanxi Key Laboratory of Petroleum Accumulation Geology (PAG-2021-02), Open Funds of the Key Laboratory of Tectonics and Petroleum Resources (China University of Geosciences) (TPR-2021-02), Fundamental Research Funds for the Central Universities (20CX06085A), and Qingdao Postdoctoral (ZX20210070).

Nomenclature and glossary

OS	Oil saturation
WS	Water saturation
φ_{He}	Porosity obtained by He method, %
φ_{os}	Porosity obtained by oil saturation method, %
ρ_o	Density of saturating oil, g/cm^3
ρ_k	Density of kerogen, g/cm^3
ρ_b	Bulk density of shale sample, g/cm^3
V	Bulk volume of sample, cm^3
m_1	Dried shales weighed, g
m_2	Oil-saturated shales weighed, g
H_1	Initial height of kerogen in kerogen-dissolve oil experiment, mm
H_2	Height of kerogen after centrifuge, mm
Q_v	Kerogen swelling ratio
TOC	Total organic carbon, w.t.%
TOC_k	Total organic carbon content of kerogen, w.t.%
R_o	Vitrinite reflectance, %
M_d	Dissolved oil content of kerogen, g oil/g TOC
$\varphi_{os\text{-}c}$	Corrected porosity obtained by the saturated oil method, %

References

Ai, T., Wu, S.Y., Zhang, R., et al., 2021. Changes in the structure and mechanical properties of a typical coal induced by water immersion. Int. J. Rock Mech. Min. Sci. 138, 104597. https://doi.org/10.1016/j.ijrmms.2020.104597.

Al Hinai, A., Rezaee, R., Esteban, L., et al., 2014. Comparisons of pore size distribution: a case from the Western Australian gas shale formations. J. Unconventional Oil. Gas Resour. 8, 1–13. https://doi.org/10.1016/j.juogr.2014.06.002.

Anovitz, L.M., Cole, D.R., 2015. Characterization and analysis of porosity and pore structures. Rev. Mineral. Geochem. 80, 61–164. https://doi.org/10.2138/rmg.2015.80.04.

Bai, L.H., Liu, B., Du, Y.J., et al., 2022. Distribution characteristics and oil mobility thresholds in lacustrine shale reservoir: insights from N2 adsorption experiments on samples prior to and following hydrocarbon extraction. Petrol. Sci. 19, 486–497. https://doi.org/10.1016/j.petsci.2021.10.018.

Bhandari, A.R., Flemings, P.B., Ramiro-Ramirez, S., et al., 2019. Gas and liquid permeability measurements in Wolfcamp samples. Fuel 236, 1026–1036. https://doi.org/10.1016/j.fuel.2018.09.038.

DiStefano, V.H., McFarlane, J., Stack, A.G., et al., 2019. Solvent-pore interactions in the Eagle Ford shale formation. Fuel 238, 298–311. https://doi.org/10.1016/j.fuel.2018.10.010.

Gannaway, G., 2014. NMR investigation of pore structure in gas shales. In: SPE Annual Technical Conference and Exhibition. https://doi.org/10.2118/173474-STU.

Zhu, C.F, Sheng, J.J., Ettehadtavakkol, A., et al., 2020. Numerical and experimental study of oil transfer in laminated shale. Int. J. Coal Geol. 217, 103365. https://doi.org/10.1016/j.coal.2019.103365.

GB/T19144-2010, Isolation Method for Kerogen from Sedimentary Rock (in Chinese).

GB/T34533-2017, Measurement of Helium Porosity and Pulse Decay Permeability of Shale (in Chinese).

Gong, H.J., Zhu, C.F., Zhang, Y.L., et al., 2020. Experimental evaluation on the oil saturation and movability in the organic and inorganic matter of shale. Energy Fuel. 34, 8063–8073. https://doi.org/10.1021/acs.energyfuels.0c00831.

Handwerger, D.A., Suarez-Rivera, R., Vaughn, K., et al., 2011. Improved petrophysical core measurements on tight shale reservoirs using retort and crushed samples. In: SPE Annual Technical Conference and Exhibition. https://doi.org/10.2118/147456-MS.

Jarvie, D.M., 2014. Components and processes affecting producibility and commerciality of shale resource systems. Geol. Acta: Int. Earth Sci. J. 12, 307–325. https://doi.org/10.1344/GeologicaActa2014.12.4.3.

Josh, M., Esteban, L., Delle Piane, C., et al., 2012. Laboratory characterisation of shale properties. J. Petrol. Sci. Eng. 88, 107–124. https://doi.org/10.1016/j.petrol.2012.01.023.

Kausik, R., Fellah, K., Rylander, E., et al., 2014. NMR Petrophysics for Tight Oil Shale Enabled by Core Resaturation. International Symposium of the Society of Core Analysts, Avignon, France, pp. 8–11.

Kelemen, S., Walters, C., Ertas, D., et al., 2006. Petroleum expulsion part 2. Organic matter type and maturity effects on kerogen swelling by solvents and thermodynamic parameters for kerogen from regular solution theory. Energy Fuel. 20, 301–308. https://doi.org/10.1021/ef0580220.

Kuila, U., McCarty, D.K., Derkowski, A., et al., 2014. Total porosity measurement in gas shales by the water immersion porosimetry (WIP) method. Fuel 117, 1115–1129. https://doi.org/10.1016/j.fuel.2013.09.073.

Larsen, J.W., Parikh, H., Michels, R., 2002. Changes in the cross-link density of Paris Basin Toarcian kerogen during maturation. Org. Geochem. 33, 1143–1152. https://doi.org/10.1016/S0146-6380(02)00102-X.

Li, J.B., Lu, S.F., Chen, G.H., et al., 2019a. A new method for measuring shale porosity with low-field nuclear magnetic resonance considering non-fluid signals. Mar. Petrol. Geol. 102, 535–543. https://doi.org/10.1016/j.marpetgeo.2019.01.013.

Li, J.B., Lu, S.F., Jiang, C.Q., et al., 2019b. Characterization of shale pore size distribution by NMR considering the influence of shale skeleton signals. Energy Fuel. 33, 6361–6372. https://doi.org/10.1021/acs.energyfuels.9b01317.

Liu, B., Shi, J.X., Fu, X., et al., 2018. Petrological characteristics and shale oil enrichment of lacustrine fine-grained sedimentary system: a case study of organic-rich shale in first member of Cretaceous Qingshankou Formation in Gulong Sag, Songliao Basin, NE China. Petrol. Explor. Dev. 45, 884–894. https://doi.org/10.1016/S1876-3804(18)30091-0.

Luffel, D., Guidry, F., 1992. New core analysis methods for measuring reservoir rock properties of Devonian shale. J. Petrol. Technol. 44, 1184–1190. https://doi.org/10.2118/20571-PA.

Milliken, K.L., Rudnicki, M., Awwiller, D.N., et al., 2013. Organic matter–hosted pore system, Marcellus formation (Devonian), Pennsylvania. AAPG Bull. 97, 177–200. https://doi.org/10.1306/07231212048.

Ousseini Tinni, A., 2015. Pore Connectivity and Hydrocarbon Storage in Shale Reservoirs. University of Oklahoma.
Ritter, U., 2003. Solubility of petroleum compounds in kerogen: implications for petroleum expulsion. Org. Geochem. 34, 319–326. https://doi.org/10.1016/S0146-6380(02)00245-0.
Saidian, M., Kuila, U., Rivera, S., et al., 2014. Porosity and pore size distribution in mudrocks: a comparative study for haynesville, niobrara, monterey and eastern European silurian formations. In: SPE/AAPG/SEG Unconventional Resources Technology Conference. https://doi.org/10.15530/urtec-2014-1922745.
Sandvik, E., Young, W., Curry, D., 1992. Expulsion from hydrocarbon sources: the role of organic absorption. Org. Geochem. 19, 77–87. https://doi.org/10.1016/0146-6380(92)90028-V.
Sang, Q., Zhang, S.J., Li, Y.J., et al., 2018. Determination of organic and inorganic hydrocarbon saturations and effective porosities in shale using vacuum-imbibition method. Int. J. Coal Geol. 200, 123–134. https://doi.org/10.1016/j.coal.2018.10.010.
Sun, J.N., Liang, T., Lin, X.H., et al., 2019. Oil generation and retention kinetics from the upper Es4 source rock in the Dongying Depression. Geochimica 48, 370–377. https://doi.org/10.19700/j.0379-1726.2019.04.005.
Topór, T., Derkowski, A., Kuila, U., et al., 2016. Dual liquid porosimetry: a porosity measurement technique for oil-and gas-bearing shales. Fuel 183, 537–549. https://doi.org/10.1016/j.fuel.2016.06.102.
Wang, M., Ma, R., Li, J.B., et al., 2019. Occurrence mechanism of lacustrine shale oil in the paleogene shahejie formation of jiyang depression, Bohai Bay basin, China. Petrol. Explor. Dev. 46, 833–846. https://doi.org/10.1016/S1876-3804(19)60242-9.
Wei, Z.F., Zou, Y.R., Cai, Y.L., et al., 2012. Kinetics of oil group-type generation and expulsion: an integrated application to Dongying Depression, Bohai Bay Basin, China. Org. Geochem. 52, 1–12. https://doi.org/10.1016/j.orggeochem.2012.08.006.
Yang, F., Ning, Z.F., Wang, Q., et al., 2016. Pore structure characteristics of lower Silurian shales in the southern Sichuan Basin, China: insights to pore development and gas storage mechanism. Int. J. Coal Geol. 156, 12–24. https://doi.org/10.1016/j.coal.2015.12.015.
Zargari, S., Canter, K.L., Prasad, M., 2015. Porosity evolution in oil-prone source rocks. Fuel 153, 110–117. https://doi.org/10.1016/j.fuel.2015.02.072.
Zhang, P.F., Li, J.Q., Lu, S.F., et al., 2017. A precise porosity measurement method for oil-bearing micro/nano porous shales using low-field nuclear magnetic resonance (LF-NMR). J. Nanosci. Nanotechnol. 17, 6827–6835. https://doi.org/10.1166/jnn.2017.14518.
Zhang, S.J., Li, Y.H., Pu, H., 2020. Studies of the storage and transport of water and oil in organic-rich shale using vacuum imbibition method. Fuel 266, 117096. https://doi.org/10.1016/j.fuel.2020.117096.
Zhao, P., He, B., Zhang, B., et al., 2021. Porosity of gas shale: Is the NMR-based measurement reliable? Petrol. Sci. https://doi.org/10.1016/j.petsci.2021.12.013.
Zhou, S.W., Dong, D.Z., Zhang, J.H., et al., 2021. Optimization of key parameters for porosity measurement of shale gas reservoirs. Nat. Gas. Ind. B 8, 455–463. https://doi.org/10.1016/j.ngib.2021.08.004.